Transaction

Photocatalytic Activity of Titanium Oxide Nano-Networks Fabricated through Organogel Route Using L-Isoleucine-Based Gelator

Masahiro Suzuki#, Masahiro Kikuchi, and Kenji Hanabusa

Graduate School of Science and Technology, Shinshu University, Ueda, Nagano 386-8567, Japan

Abstract: Titanium oxide nano-networks, which have various crystal structures, were fabricated by the sol-gel polymerization in an organogel formed by L-isoleucine organogelator and their photocatalytic activities were evaluated by a methylene blue method. The TiO_2 nano-networks were formed by which the self-assembled nanofibers of the gelator acted as a template, and their crystal structure was controlled by the calcination temperature. The rutile TiO_2 nano-network, which was fabricated at 700°C, showed a good photocatalytic activity.

(Received 13 May, 2014 ; Accepted 26 June, 2014)

1. Introduction

Semiconducting photocatalysts have attracted much attention in recent years because of their applications related to environment and energy [1,2]. Particularly, titanium oxide (TiO_2) is one of the promising materials because of its good photoreactivity, nontoxicity, stability and low cost [3]. The photocatalytic performance of TiO_2 is primary determined by its physicochemical properties such as crystal structure, shape, size, surface area and crystallinity [3-5]. In the preparation of nanostructured TiO_2, the control of these properties, especially of crystal structure and surface area represents some of the important issues in this area.

There have been many reports on the synthesis of nanostructured TiO_2 using sol-gel [6-8], micelle [9,10], polyol,[11], sonochemical synthesis [12], hydrothermal method [13,14], and so on [3,15-17]. Template-directed synthesis using titanium alkoxides as the TiO_2 precursor is widely accepted as a simple and cost-effective method for the fabrication of TiO_2 through the sol-gel polymerization. Recently, the use of low-molecular-weight gelators as the organic templates for template-directed synthesis have been investigated [18-23]. Because the low-molecular-weight gelators produce various nanostructures such as nanofibers, nanoribbons, nanorods, and nanoparticles in the organogels, many low-molecular-weight gelators have been recognized as one of the good organic templates [24-32]. We reported the fabrication of nanostructured TiO_2 using low-molecular-weight gelators ; e.g., TiO_2 nanotubes, nanoparticles and helical TiO_2 nanotubes [33-35]. In this letter, we describe the fabrication of TiO_2 nano-networks using the L-isoleucine-based gelator (Fig. 1), and the evaluation of their photocatalytic activities using the methylene blue (MB) method.

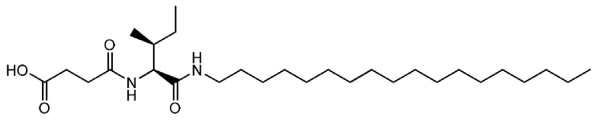

Fig. 1 Chemical structure of L-isoleucine-based gelator.

2. Experimental

2.1 Materials

L-Isoleucine-based gelator was prepared according to the literature [36]. The other chemicals were of the highest commercially available grade and used without further purification. All solvents used in the syntheses were purified, dried, or freshly distilled as required.

2.2 Fabrication of nanostructured TiO_2.

The nanostructured TiO_2 (nano-networks and nanoparticles) were fabricated according to the literature [33-35]. The typical procedure was as follows. L-Isoleucine-based gelator (20 mg), $[Ti(OiPr)_4]$ (1.5 mL) and propylamine (6.7 μL) as a catalyst were dissolved in 1,4-dioxane (0.85ml), and then the solution was cooled to room temperature, leading to the formation of an organogel. The resulting gel was allowed to stand at 25°C for 5 days. After washing with $CHCl_3$, the white solid was dried at 50°C in vacuum overnight. The white powder of TiO_2 was obtained by calcination at 200°C for 2h and then various temperatures (400-1000°C) for 2h.

corresponding author

2.3 Instrumentation

The elemental analyses were performed using a Perkin-Elmer series II CHNS/O analyzer 2400. The FT-IR spectra were recorded on a JASCO FS-420 spectrometer. The field emission scanning electron microscopy (FE-SEM) was carried out using a Hitachi S-5000 field emission scanning electron microscope. ^{1}H-NMR spectra were measured using a Bruker AVANCE 400 spectrometer with TMS as the standard. The UV-Vis absorption spectra were measured using a JASCO V-570 UV / VIS / NIR spectrophotometer. Products were characterized by powder X-ray diffraction using Cu Kα radiation (λ = 1.5418 Å) at 40 kV and 150 mA in a range of 3-60º on a Rigaku wide-angle X-ray diffractometer type Rad-rX. The BET (Brunauer-Emmett-Teller) surface area was measured using nitrogen adsorption on a Shimadzu Gemini2375.

2.4 Photocatalytic activity

The photocatalytic reactions were carried out at 25ºC using a home-made reactor that contains two UV lamps (8W x 2, characteristic wavelength = 365 nm) mounted 5 cm away from the reaction solution (light intensity = 1820 μW cm^{-2}). TiO_2 (10 mg) was mixed with 50 ml aqueous solution (pH = 6-7) containing 3.13 x 10^{-5} M MB. After the ultrasonic treatment for 1 h and then stirring for 1 h under the dark condition, the UV light was irradiated while stirring. During UV irradiation, a small part of the solution was withdrawn periodically, and the TiO_2 powder was immediately filtered by using syringe filter (pore size 0.1 μm and diameter 10 mm). The filtrate was analyzed to determine the residual concentration of MB with a UV-Vis spectrometer (monitoring at 664 nm that is the maximum wavelength of MB with 68,200 of molar absorption coefficient). Preliminary studies indicated no decomposition of MB in the absence of TiO_2 under UV irradiation. The reproducibility was checked by repeating the measurements at least three times and was found to be within the acceptable range (±5%).

3. Results and discussion

3.1 Gelation property and nanostructure

L-isoleucine-based gelator acts as a good organogelator that form the organogels in many organic fluids through the creation of three-dimensional networks. The FE-SEM images of dried samples prepared from 1,4-dioxane gels based on the L-isoleucine-based gelator (30 mg/L) demonstrated that these gelators created a three-dimensional network formed by the entanglement of self-assembled nanofibers with a diameter of 40-100 nm.

3.2 TiO_2 Nano-Networks

The sol-gel polymerization to form the gel of L-isoleucine-based gelator in 1,4-diaoxane containing titanium tetraisopropoxide [$Ti(OiPr)_4$] and propylamine as a catalyst produced the TiO_2 nano-networks. When the sol-gel polymerization was carried out without gelators, the TiO_2 particles, which had a diameter of several micrometers and wide distribution of the diameters, were fabricated. Fig. 2 shows the FE-SEM images of the dried gel of L-isoleucine-based gelator prepared from the 1,4-dioxane gel and the TiO_2 nano-network fabricated in the gel of L-isoleucine-based gelator. The TiO_2 nano-network is similar to the nano-structure created by L-isoleucine-based gelator in gel. This result indicates that the gel fibers of L-isoleucine-based gelator act as the effective template. It is generally known that some interactions between the gel fibers and TiO_2 precursors are very important for template-directing sol-gel polymerization and an electrostatic interaction is often used [34-36]. We previously reported the fabrication of TiO_2 nanotubes using L-lysine gelators [34]. In the present case, the sol-gel polymerization proceeds the similar mechanism ; partial propylamine used as a catalyst for the sol-gel polymerization reacts with the carboxyl groups in the L-isoleucine-based gelator. The TiO_2 precursors (negatively charged) are attracted to the charged nanofibers and the sol-gel polymerization occurs on the gel fibers. Most of the TiO_2 nano-networks consists of the nanowire, but the TEM observation showed the part of TiO_2 nanowires has a nanotube structure with an inside diameter less than a few nanometers. This fact may indicate that the nanowire is formed by shrinking of tubes during calcination.

3.3 Effect of calcination temperatures

The calcination temperature influences the nanostructure of TiO_2. Fig. 3 shows the FE-SEM images of the TiO_2 nano-networks fabricated at different calcination temperatures. The TiO_2 nano-networks were

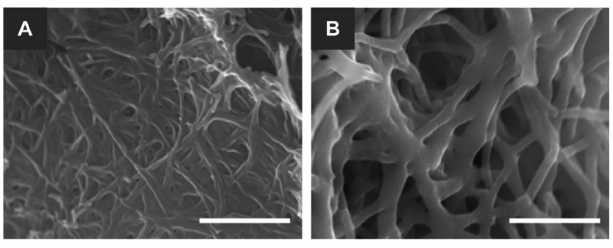

Fig. 2 FE-SEM images of dried gel of L-isoleucine-based gelator prepared from 1,4-dioxane gel (A) and TiO_2 nano-networks (B) fabricated in 1,4-dioxane gel containing [Gelator] = 20 mg (41 μmol), [$Ti(OiPr)_4$] = 0.15 ml (510 μmol), [$C_3H_7NH_2$] = 6.7 μl and 0.85 ml of 1,4-dioxane. Scale bars are 1.2 μm.

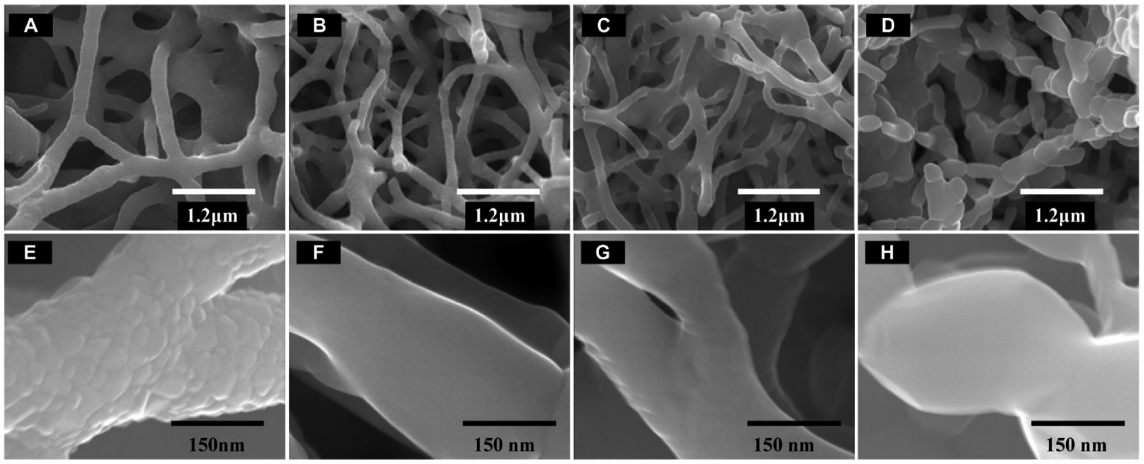

Fig. 3 FE-SEM images of TiO_2 nano-networks prepared at different calcination temperatures. Calcination temperatures are 650 ºC for A and E, 700 ºC for B and F, 800 ºC for C and G, and 900 ºC for D and H.

retained up to 800ºC (images A-C) and the TiO_2 nanofibers forming the nano-networks was decomposed over 800ºC. The TiO_2 calcinated at 900 °C had a necklace structure (image D) and was no longer a nanofiber. Furthermore, the surface morphology of the TiO_2 nanofibers was uneven up to 650ºC, and changed to the smooth surface above 700°C of calcination temperature. The calcination temperature affects not only the nanostructure of TiO_2 but also the crystal phase structure. The XRD measurement is used to identify the phase of the TiO_2 nano-networks. In general, TiO_2 has two main phases, anatase, which can be kinetically favored over rutile, the thermodynamically stable phase. Fig. 4 shows the powder X-ray diffraction patterns of TiO_2 nano-networks fabricated at different calcination temperatures. The TiO_2 nano-networks, which were calcinated below 550°C, had the crystal phase structure of anatase, while the calcination temperatures above 700°C produced the rutile TiO_2 nano-networks. The TiO_2 nano-networks having the mixed phase structure of anatase and rutile were obtained at calcination temperatures of 600 and 650°C. Considering the results in the FE-SEM, the change in the morphology from uneven to smooth surfaces is induced by the change in the crystal phase structure from anatase to rutile. It is noteworthy that the rutile TiO_2 nano-networks are formed at 700-800ºC with maintaining the nanostructure. At the high calcination temperature, the TiO_2 nanofibers are sintered by calcination and decomposed to the necklace structure.

Furthermore, the surface areas decreased with increasing calcination temperatures. This is because the crystalline phase was changed from anatase into rutile and the surface becomes smooth.

3.4 Photocatalytic activity

The photocatalytic activities of the TiO_2 nano-networks were evaluated by the methylene blue (MB) method at 25ºC [37]. The data of the photocatalytic activities (decomposition of MB after UV irradiation for 4h using the TiO_2 nano-networks), surface areas, crystal structures, surface morphologies and nanostructures of TiO_2 nano-networks are listed in Table 1. The photocatalytic activity of the TiO_2 nano-networks

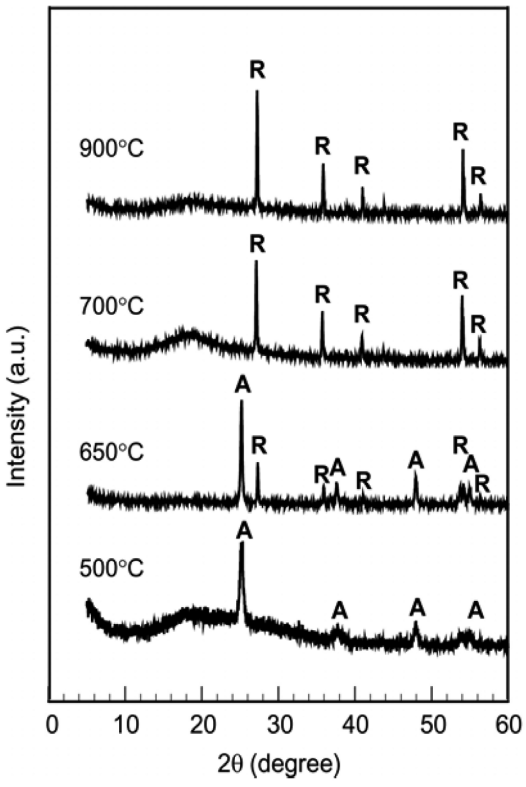

Fig. 4 XRD patterns of TiO_2 nano-networks fabricated at different calcination temperatures. A is anatase and R is rutile.

Table 1 Photocatalytic activities, crystal structures, surface morphologies and nanostructures of TiO_2 nano-networks.

sample	Calcination temperature	Surface area	Activity	Crystal	Surface	Nanostructure
N1	400°C	11.3	18%	A	Uneven	Networks
N2	500°C	9.8	24%	A	Uneven	Networks
N3	550°C	8.8	30%	A	Uneven	Networks
N4	600°C	8.7	36%	A/R	Uneven	Networks
N5	650°C	7.3	38%	A/R	Uneven	Networks
N6	700°C	5.2	49%	R	Smooth	Networks
N7	750°C	2.2	42%	R	Smooth	Networks
N8	800°C	1.3	38%	R	Smooth	Networks
N9	900°C	1.2	36%	R	Smooth	Sintering
N10	1000°C	1.0	30%	R	Smooth	Sintering

BET surface areas ($m^2 \cdot g^{-1}$). Activity is degradation of MB by UV light irradiation for 4h. A : anatase ; R : rutile.

significantly depended on the calcination temperature and the crystal phase structure. The degradation of MB increased with increasing the calcination temperature and then decreased via the maximum value at 700°C. Moreover, the photocatalytic activity remarkably decreased for the TiO_2 calcinated above 900°C. As shown in Fig. 3, the calcination above 900°C of the TiO_2 decomposes the nano-network structure due to sintering of the TiO_2 nanofibers, thus leading to the decrease in the photocatalytic activity. Such the trend of the photocatalytic activity demonstrated that the activity depended on at least two factors ; probably, surface area and promotion of the charge separation of electron-hole pairs [1-3]. Namely, the decrease in the surface areas should decrease the activity, while the rutile phase may promote the charge separation. As a result, the TiO_2 nano-network, which is fabricated at 700°C and has the rutile crystal structure, showed the best photocatalytic activity. Compared with sample N3 (anatase), the sample N5, which has a mixed crystal phase structure of rutile and anatase, and sample N8 (rutile) can decompose the more MB, indicating that the rutile TiO_2 nano-network is superior to anatase one. These results imply that the photocatalytic activity of the TiO_2 nano-networks significantly depends on the nanostructure and the crystal phase structure.

4. Conclusion

We revealed the fabrication of TiO_2 nano-network through the organogel route using L-isoleucine-based organogelator as the organic templates. The sol-gel polymerization in 1,4-dioxane gels of L-isoleucine-based gelator produces the TiO_2 nano-network due to the template transcription of the self-assembled nanofibers of L-isoleucine-based gelator. The nanostructure and crystal phase structure depend on the calcination temperature, and the TiO_2 nano-network is structurally stable and its nano-network structure retains up to the calcination temperature at 800°C. It is noteworthy that the rutile TiO_2 nano-network is obtained by calcination temperature at 700-800°C. The photocatalytic activity of the TiO_2 nano-networks significantly depend on its nanostructure and crystal phase structure, and the rutile TiO_2 nano-network prepared by the calcination temperature at 700°C shows the best photocatalytic activity.

References and notes

1. MR. Hoffmann, S. T. Martin, W. Y. Choi and D. W. Bahnemann, *Chem. Rev*., **95**, 69 (1995).
2. T. L. Thompson and J. T. Yates, *Chem. Rev*., **106**, 4428 (2006).
3. X. Chen and S. S. Mao, *Chem. Rev*., **107**, 2891 (2007).
4. D. He and F. Lin, *Mater. Lett*., **61**, 3385 (2007).
5. G. H. Tian, H. G. Fu, L. Q. Jing, B. F. Xin and K. Pan, *J. Phys. Chem. C*, **112**, 3083 (2008).
6. T. Moritz, J. Reiss, K. Diesner, D. Su and A. Chemseddine, *J. Phys. Chem. B*, **101**, 8052 (1997).
7. A. S. Pottier, S. Cassaignon, C. Chaneac, F. Villain, E. Tronc and J. P. Jolivet, *J. Mater. Chem*., **13**, 877 (2003).
8. M. H. Bartl, S. W. Boettcher, K. L. Frindell and G. D. Stucky, *Acc. Chem. Re*s., **38**, 263 (2005).
9. D. B. Zhang, L. M. Qi, J. M. Ma and H. M. Chen, *J. Mater. Chem*., **12**, 3677 (2002).
10. Y. Z. Li, N. H. Lee, D. S. Hwang, J. S. Song, E. G. Lee and S. J. Kim, *Langmuir*, **20**, 10838 (2004).
11. C. Feldmann and H. O. Jungk, *Angew. Chem. Int. Ed*., **40**, 359 (2001).
12. J. C. Yu, J. G. Yu, W. K. Ho and L. Z. Zhang, *Chem.*

Commun., 1942 (2001).
13. R. R. Bacsa and M. Grätzel, *J. Am. Ceram. Soc*., **79**, 2185 (1996).
14. X. L. Li, Q. Peng, J. X. Yi, X. Wang and Y. D. Li, *Chem. Eur. J*., **12**, 2383 (2006).
15. P. D. Cozzoli, A. Kornowski and H. Weller, *J. Am. Chem. Soc*., **125**, 14539 (2003).
16. Z. H. Zhang, X. H. Zhong, S. H. Liu, D. F. Li and M. Y. Han, *Angew. Chem. Int. Ed*., **44**, 3466 (2005).
17. M. Niederberger, *Acc. Chem. Res*., **40**, 793 (2007).
18. Y. Ono, K. Nakashima, M. Sano, Y. Kanekiyo, K. Inoue, J. Hojo and S. Shinkai, *Chem. Commun*., 1477 (1998).
19. J. H. Jung, Y. Ono, K. Hanabusa and S. Shinkai, *J. Am. Chem. Soc*., **122**, 5008 (2000).
20. J. H. Jung, S. Shinkai and T. Shimizu, *Chem. Rev*., **103**, 212 (2003).
21. T. Shimizu, M. Masuda and H. Minamikawa, *Chem. Rev*., **105**, 1401 (2005).
22. Y. Yang, M. Suzuki, M. Kimura, H. Shirai and K. Hanabusa, *Chem. Commun*., 1332 (2004).
23. Y. Yang, M. Suzuki, M. Kimura, H. Shirai, A. Kurose and K. Hanabusa, *Chem. Commun*., 2032 (2005).
24. R. G. Weiss and P. Terech ; Eds., *Molecular Gels : Materials with Self-Assembled Fibrillar Networks*, Dordrecht, Springer, (2006).
25. F. Fages ; Ed., Top. Curr. Chem. 256, *Low Molecular Mass Gelators : Design, Self-assembly, Function*, New York, Springer, (2005).
26. P. Terech and R. G. Weiss, *Chem. Rev*., **97**, 3133 (1997).
27. J. H. van Esch, R. M. Kellogg and B. L. Feringa, *Angew. Chem. Int. Ed*., **39**, 2263 (2000).
28. L. A. Estroff and A. D. Hamilton, *Chem. Rev*., **104**, 1201 (2004).
29. N. Sangeetha and U. Maitra, *Chem. Soc. Rev*., **34**, 821 (2005).
30. M. George and R. G. Weiss, *Acc. Chem. Res*., **39**, 489 (2006).
31. P. Dastidar, *Chem. Soc. Rev*., **37**, 2699 (2009).
32. M. Suzuki and K. Hanabusa, *Chem. Soc. Rev*., **38**, 967 (2009).
33. S. Kobayashi, N. Hamasaki, M. Suzuki, M. Kimura, H. Shirai and K. Hanabusa, *J. Am. Chem. Soc*., **124**, 6550 (2002).
34. M. Suzuki, Y. Nakajima, T. Sato, H. Shirai and K. Hanabusa, *Chem. Commun*., 377 (2006).
35. K. Hanabusa, T. Numazawa, S. Kobayashi, M. Suzuki and H. Shirai, *Macromol. Symp*., **235**, 52 (2006).
36. M. Suzuki, T. Sato, H. Shirai and K. Hanabusa, *New J. Chem*., **30**, 1184 (2006).
37. G. H. Kim, B. -K. Kim and K. S. Yang, *Syn. Met*., **161**, 1068 (2011).